ISBN: 978-3-95450-227-1 ISSN: 2673-5490 doi:10.18429/JACoW-IPAC2022-TUPOPT065

DISPERSION-FREE STEERING BEAM BASED ALIGNMENT AT SwissFEL

Eugenio Ferrari*, Marco Calvi, Romain Ganter, Christoph Kittel[1], Eduard Prat, Sven Reiche, Thomas Schietinger, Paul Scherrer Institut, CH-5232 Villigen PSI, Switzerland
[1]also at Faculty of ICT, University of Malta, Msida MSD 2080, Malta

Abstract

Micron-level alignment of the undulator line is required for successful operation of linear accelerator based high gain free electron lasers to produce powerful radiation at X-rays' wavelengths. Such precision in the straightness of the trajectory allows for an optimal transverse superposition between the electrons and the photon beam. This is extremely challenging and can only be achieved via beam-based techniques. In this paper we will report on the dispersion-free steering approach implemented at SwissFEL, that helped achieving improved performance for both the hard and soft X-ray beamlines.

INTRODUCTION

SwissFEL [1] is a free-electron laser (FEL) user facility, based on the SASE principle, delivering ultrashort photon pulses in the X-ray regime. For a schematic representation of the facility, see Fig. 1. The electrons needed for FEL production are generated in a normal conducting photocathode gun and accelerated through a normal conducting linac. The gun and booster sections, before the first bunch compressor, employ S-band technology. All the other accelerating cavities, divided for convenience into 4 linacs, are at C-band frequency. Two magnetic chicanes are used to compress the pulse duration. An X-band harmonic cavity is also installed and used to linearise the phase space before compression.

Two different photoinjector lasers are used to generate two electron bunches with temporal separation of 28 ns. This allows parallel operation of two distinct FEL beamlines. The electrons of bunch 1 are accelerated to the required energy and injected in the Aramis undulator, for hard-X-ray generation in the 2–12 keV photon energy range. The typical electron beam energies are 3–6 GeV, depending on the requirement of the specific user experiment. Bunch 2 electrons are extracted after Linac 2, using a combination of resonant kicker and septum, and they are injected at 3 GeV in the Athos branch for soft-X-ray production. The photon energy range of the second beamline is 0.25–1.9 keV. Both beamlines can operate in parallel at a full repetition rate of 100 Hz.

The Aramis undulator [1] consists of 13 in-vacuum variable-gap modules, each 4 m-long, interleaved with 0.75 m break sections containing a sub-μm resolution BPM, a quadrupole magnet and a phase shifter. Athos [2] on the other hand consists of 16 out-of-vacuum Apple-X modules of 2 m length with break lengths of 0.8 m, housing a CHIC-chicane instead of the phase shifter [3]. Each quadrupole/BPM pair is mounted on a remotely controlled plate with travel range of 1 mm in the horizontal and vertical planes for alignment purposes in both the Aramis and Athos undulator beamlines. The BPM offsets relative to the centre of the quadrupoles can be corrected via software. The undulator modules can also be remotely aligned, in the horizontal and vertical plane, both in offset and angle.

To achieve best lasing performance in a reproducible way, the alignment of the quadrupole magnets is critical. The electron and photon beams must be transversally superimposed inside the undulator for efficient FEL amplification. The maximum allowed transverse misalignments should be better than 10 μm. Such extreme tolerances are not achievable using traditional alignment techniques (tunnel survey), hence it is necessary to implement beam-based alignment (BBA) techniques.

PROCEDURE

Originally developed for the LCLS [4] and successfully demonstrated at PAL [5] and EuXFEL [6], the dispersion-free steering BBA is a procedure that allows finding a straight electron beam trajectory along the undulator line. The straightness of the trajectory inside each of the undulator module relies instead on the correct compensation of first and second field integrals, corrected using dedicated coils set according to feed-forward tables. The procedure allows the reconstruction of the position of the quadrupoles with respect to a straight line as well as the offsets of the BPMs by measuring and minimising the dispersion along the beamline. It is based on measuring the electron beam trajectories for widely different energies in order to distinguish between magnetic kicks, caused by quadrupole offsets or other spurious kicks, which scale linearly with energy, and BPM offsets, which are energy independent [4, 5]. Critical for the success of the procedure is that the transport optics till the entrance of the beamline stays constant when changing energy, while nothing must be changed in the undulator beamline.

In the case of SwissFEL, for such wide energy changes we follow different strategies depending on the beamline. In the case of Aramis, we put off timing the RF of successive accelerating cavities in Linac 3, see Fig. 1, such that the beam energy is varied from 5.9 GeV to 3 GeV. We usually consider four energy steps, equally spaced in inverse electron beam energy, such that the strength of the quadrupole magnets varies by the same amount (while staying at the same current). In the case of Athos, we change the acceleration settings of Linac 2, see Fig. 1, while compensating the

* eugenio.ferrari@psi.ch

This is a preprint — the final version is published with IOP

Content from this work may be used under the terms of the CC BY 4.0 licence (© 2022). Any distribution of this work must maintain attribution to the author(s), title of the work, publisher, and DOI

ISBN: 978-3-95450-227-1 ISSN: 2673-5490 doi:10.18429/JACoW-IPAC2022-TUPOPT065

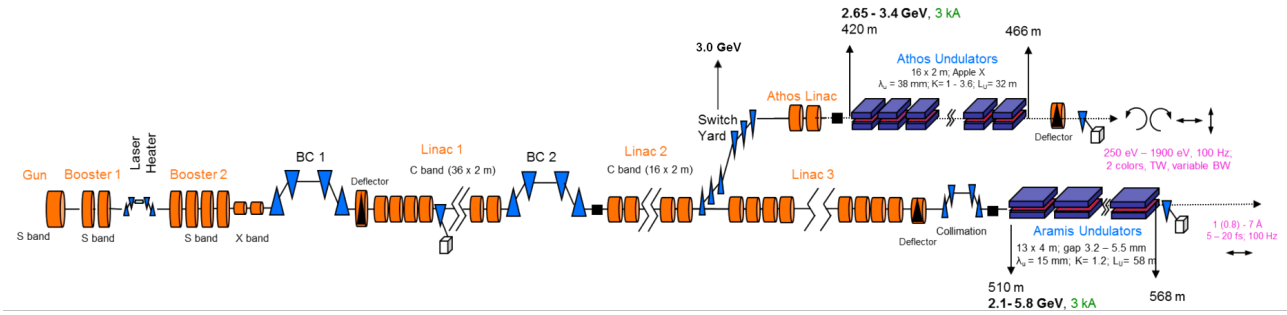

Figure 1: Schematic overview of the SwissFEL accelerator and FEL lines. Design parameters are also shown, as well as the typical operation energies for the different sections. Two bunches, separated by 28 ns, are generated at the gun using two different photoinjector lasers. The first bunch is sent to the Aramis beamline (hard X-rays), while the second bunch is extracted after Linac 2 using a resonant kicker and septum and, through a switchyard, injected into the Athos beamline (soft X-rays). Image reproduced from [7].

energy change using Linac 3 to maintain lasing in Aramis. This allows for the beam based feedbacks, mostly acting on bunch 1, to keep stable the transverse and longitudinal beam properties for both bunches in the common part of the machine.

In the case of Athos we vary the beam energy between 3 GeV and 2 GeV. In the future, it will be possible to use the dedicated C-band station at the beginning of the Athos beamline also for the BBA, although with reduced energy variation (±250 MeV). For both beamlines we go from higher to lower energy settings. At each energy, we save the machine settings to have a faster set-up in successive iterations of the BBA procedure. Together with appropriate cycling of the magnets, such a strategy allows for better reproducibility of the measurement conditions, which in turn help the convergence of the procedure. The BBA is now routinely performed with the gaps of the undulators closed. It was only done with open undulators at the beginning, to establish reasonable starting conditions and minimise the deposited radiation dose on the devices.

For a successful BBA, injection offset and angular errors, coming from the upstream Linac, must be evaluated and corrected. Our approach is to use two pairs of steering magnets, one for each plane, installed on two quadrupoles preceding the part of the undulator beamline for which the BBA is applied, to correct the trajectory along the full undulator line. This is performed either temporarily modifying the settings of the trajectory feedback or using dedicated trajectory correction tools. We ignore the readings of the two BPMs attached to these two quadrupole magnets in this phase.

At the end of the BBA, the offsets of the launch BPMs are adapted so that they read zero and the corresponding quadrupoles are moved to minimise the corrector current, thus achieving an appropriate injection into the FEL beamline. The trajectory feedback configuration is finally restored: the correction loop runs along the full undulator line to compensate for spurious kicks from the undulators or the chicanes, when their parameters are modified, like changing the undulator gap to tune the photon energy. The full procedure requires a few hours for each of the beamlines.

RESULTS

The typical convergence of the procedure is achieved in 3 or 4 loops, with the initial one giving the largest corrections. We usually repeat the procedure until the correction amplitude is below 5 µm in the case of Aramis and 10 µm in the case of Athos.

In Fig. 2, a comparison of the results of two different BBAs, performed one year apart on the Aramis beamline, are reported. One can clearly see that the BPM offsets are very similar in the two cases (orange and red curves), once the launch region is excluded. This indicates that the relative offset between quadrupoles and BPMs is quite stable. The quadrupole positions are instead different in the two cases. This is probably due to the different quadrupole strengths in the two cases, as well as different undulator parameters. In the case of Athos, the vertical plane shows a smooth behaviour of the positions, whereas in the horizontal plane we typically observe an alternating up-down behaviour. This could be explained by residual kicks present between two quadrupoles, either due to a sign error in the correction tables for the first- and second-order integral of the undulators or the CHIC chicanes. We plan to further investigate this effect by performing dedicated BBAs with different correction signs, as well as for different polarisation settings of the undulator modules.

In Fig. 3, we report the average trajectory for the four BBA energies (a, b) and root-mean-square (rms) variation (c, d) for the Athos beamline. Panels (a, c) refer to the case before the BBA, (b, d) to the case after the BBA. The locations of the 16 undulator modules are shown as red boxes. The reduction of the trajectory variation for the different energies is clear, in particular comparing the rms before and after the BBA. The average of the rms trajectory variation is decreased from 290 µm to 4 µm for the horizontal plane, and from 93 µm to 2 µm in the vertical plane. The BPM with average significantly different from zero and rms larger than 20 µm corresponds to the location between the two kicker magnets used to correct the injection error in the beamline, which can be different for each energy. Such results clearly

Content from this work may be used under the terms of the CC BY 4.0 licence (© 2022). Any distribution of this work must maintain attribution to the author(s), title of the work, publisher, and DOI

This is a preprint — the final version is published with IOP

ISBN: 978-3-95450-227-1 ISSN: 2673-5490 doi:10.18429/JACoW-IPAC2022-TUPOPT065

demonstrate a significant reduction of the dispersion, and hence to the improved straightness of the beamline.

After proper alignment of the beamline components, a pointing correction towards the user stations can be required. It is usually performed by physically shifting all the components as a line, relying on new targets for the trajectory feedbacks for small final adjustments.

MAINTAINING RELATIVE ALIGNMENT OF QUADRUPOLES AND UNDULATORS

As reported in [5], the BBA procedure could find a bow-like solution in case of large misalignment of the undulator modules when constraints on the offsets are imposed (bounded solution). The unconstrained solution is instead immune to such bow-like solutions [5], although being characterised by larger uncertainties in the reconstruction. The behaviour is due to the quadratic dependence on energy (not linear as for quadrupolar kicks) when passing off-axis in an undulator and can lead to sub-optimal performance.

To minimise such an effect we implemented an EPICS based server, monitoring the positions of the quadrupoles (undulator follower), that adapts the position of the undulator girders, in order to maintain their relative alignment established either during the tunnel survey phase (~100 µm), or improved by photon based techniques [8].

During the December 2021 Athos BBA, we actually observed the bow formation when we tried to disable the automatic undulator follower. By comparing the bounded and unbounded solutions for the BBA inversion problem, using the same input trajectories, we noticed a significant bow-like trend for the quadrupole offsets, in particular for the horizontal plane. This was also confirmed looking at the pointing of groups of undulators on a photon imager, which confirmed the presence of the bow. This confirmed the necessity of following the movement of the quadrupoles induced by the BBA and eventual pointing corrections with the undulators, e.g., keeping the undulator follower enabled. Such an approach maintains the relative alignment between undulators and quadrupole magnets. Using the unbounded approach in January 2022, we were able to recover a bow-free trajectory, with improved transverse profile and overall better FEL performance. When comparing with the results reported in [5], the usage of short 2 m modules for Athos has the advantage of relaxing the required alignment precision, allowing us to utilise the unconstrained solution despite its larger uncertainty when compared to the constrained one.

CONCLUSION

We presented the BBA procedure and results for SwissFEL, for both the Aramis (hard X-rays) and the Athos (soft X-rays) beamline. The BBA helped establishing robust and reliable operations for both FEL beamlines. Both Aramis and Athos deliver >1 mJ photon pulse energy in their respective energy ranges. The procedure works also in the presence of spurious trajectory coupling, as observed between the horizontal and vertical plane in Athos, even though it is not explicitly included in the model. The BBA helped in obtaining good performance, as well as in improving the transverse photon beam shape. It has been fundamental in reducing or eliminating beam clipping due to the small aperture of the Athos vacuum chamber.

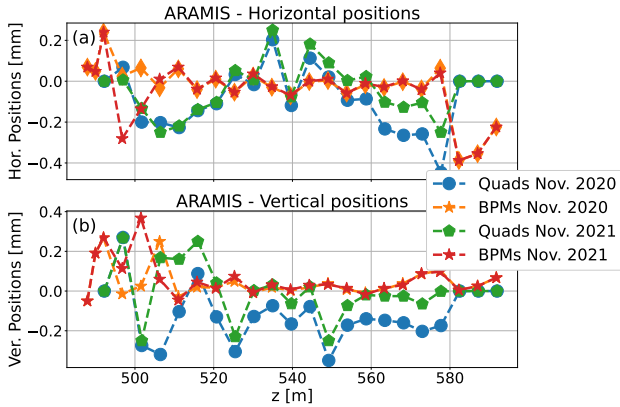

Figure 2: Horizontal (a) and vertical (b) positions of the elements along the Aramis beamline at the end of two BBA procedures, performed one year apart. One can clearly see that the BPM offsets are very similar in the two cases (orange and red curves), if the launch region is excluded. This indicates that the relative offset between quadrupoles and BPMs is quite stable. The quadrupole positions, however, are different in the two cases.

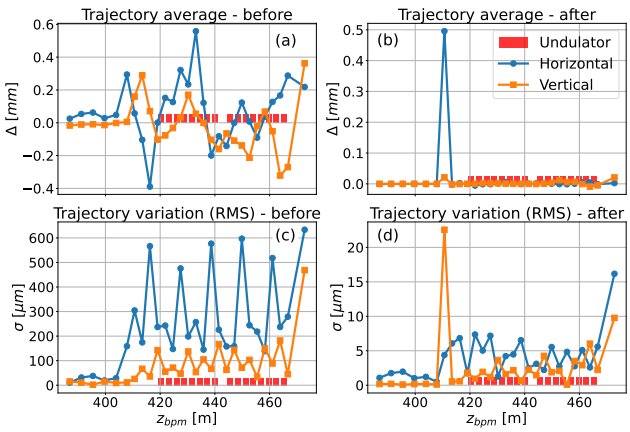

Figure 3: Average trajectory for the four BBA energies (a, b) and root-mean-square (rms) variation (c, d) for the Athos beamline. (a, c) refer to the case before the BBA, (b, d) to the case after the BBA. The locations of the 16 undulator modules are shown as red boxes. One can clearly see the reduction in the trajectory change for large energy changes, indicating a significant reduction in the dispersion, and hence in the straightness, of the beamline.

REFERENCES

[1] E. Prat *et al.*, "A compact and cost-effective hard X-ray free-electron laser driven by a high-brightness and low-energy electron beam", *Nat. Photonics*, vol. 14, pp. 748–754, 2020. doi:10.1038/s41566-020-00712-8

This is a preprint — the final version is published with IOP
Content from this work may be used under the terms of the CC BY 4.0 licence (© 2022). Any distribution of this work must maintain attribution to the author(s), title of the work, publisher, and DOI

ISBN: 978-3-95450-227-1 ISSN: 2673-5490 doi:10.18429/JACoW-IPAC2022-TUPOPT065

[2] R. Abela *et al.*, "The SwissFEL soft X-ray free-electron laser beamline: Athos", *J. Synchrotron Rad.*, vol. 26, pp. 1073–1084, 2019. doi:10.1107/S1600577519003928

[3] E. Prat *et al.*, "Undulator beamline optimization with integrated chicanes for X-ray free-electron-laser facilities", *J. Synchrotron Rad.*, vol. 23, pp. 861–868, 2016. doi:10.1107/S1600577516007165

[4] P. Emma, R. Carr, and H.-D .Nuhn, "Beam-based alignment for the LCLS FEL undulator", *Nucl. Instr. and Meth. in Phys. Res. A*, vol. 429, pp. 407–413, 1999. doi:10.1016/S0168-9002(99)00117-5

[5] H.-S. Kang and H. Loos, "X-ray free electron laser tuning for variable-gap undulators", *Phys. Rev. Accel. Beams*, vol. 22, no. 6, p. 060703, 2019. doi:10.1103/PhysRevAccelBeams.22.060703

[6] M. Scholz, W. Decking, and Y. Li, "Beam Based Alignment in all Undulator Beamlines at European XFEL", in *Proc. 39th Int. Free-Electron Laser Conf. (FEL'19)*, Hamburg, Germany, Aug. 2019, pp. 592–595. doi:10.18429/JACoW-FEL2019-THP002

[7] R. Ganter (Ed.), "Athos Conceptual Design Report", Paul Scherrer Institut, Villigen, Switzerland, PSI Rep. 17-02, Sep. 2017. https://www.dora.lib4ri.ch/psi/islandora/object/psi:34981

[8] T. Tanaka *et al.*, "Undulator commissioning by characterization of radiation in x-ray free electron lasers", *Phys. Rev. ST Accel. Beams*, vol. 15, p. 110701, 2012. doi:10.1103/PhysRevSTAB.15.110701

Content from this work may be used under the terms of the CC BY 4.0 licence (© 2022). Any distribution of this work must maintain attribution to the author(s), title of the work, publisher, and DOI

This is a preprint — the final version is published with IOP